www.czasopisma.pan.pl PAN POLSKA AKADEMIA NAUK www.journals.pan.pl

Arch. Metall. Mater. **65** (2020), 2, 805-810

DOI: 10.24425/amm.2020.132824

W. BĄK[1*], P. DULIAN[2], B. GARBARZ-GLOS[1], D. CZEKAJ[3], A. LISIŃSKA-CZEKAJ[3]

ALTERNATIVE, DIRECT SYNTHESIS METHOD OF THE CERAMIC SOLID SOLUTIONS BASED ON $BaTiO_3$ THROUGH A HIGH ENERGY BALL MILLING

Polycrystalline samples $BaTiO_3$ and the solid solutions $Ba_{0.9}Sr_{0.1}TiO_3$, $Ba_{0.9}Sr_{0.1}Ti_{0.9}Sn_{0.1}O_3$, $Ba_{0.9}Sr_{0.1}Ti_{0.8}Sn_{0.2}O_3$ were obtained by means of a mechanochemical treatment based on the high-energy ball milling technique and next a high temperature solid state reaction method. The influence of synthesis condition on microstructural, dielectric and ferroelectric properties of obtained solid solutions were investigated. The structure and morphology of the investigated samples were characterized by an X-ray diffraction (XRD) and scanning electron microscopy (SEM). The characterization of electrical properties of the ceramics within the temperature range from –130°C to 250°C were performed by means of a dielectric spectroscopy method at the frequency ranging from 0.1 Hz to 10 MHz. The diffusion of the paraelectric – ferroelectric phase transition and dielectric relaxation for ceramic samples are described.

Keywords: Ceramics, Mechanochemical synthesis, Dielectric properties, Phase transitions, Ferroelectrics

1. Introduction

The complex oxides of ABO_3-type with perovskite structure which are based on titanates in terms of applications are among the most promising classes of functional materials. Solid solutions based on $BaTiO_3$ (BT) which have a rich isomorphism are used primarily for the construction of sensors, piezoelectric transducers (actuators), non-volatile memory elements (FRAM), thermistors and multilayer ceramic capacitors of large capacity [1-2]. The dielectric properties of ceramic materials based on barium titanate depend on the concentration of ions substituted in the cationic sublattices A and/or B as well as their size and the valence [3-4]. The ions substitutions in the both cationic sublattices simultaneously generated the higher heterogeneity of structure which was confirmed by the X-ray measurements [5-6]. The differences in the sizes of ionic radii of Ba^{+2} (R_{Ba} = 0.135 nm) and Sr^{+2} (R_{Sr} = 0.118 nm) as well as Ti^{+4} (R_{Ti} = 0.061 nm) and Sn^{+4} (R_{Sn} = 0.069 nm) ions cause the changes in the size of solid solution unit cell. The substitution of Sr^{+2} ions in the cationic sublattice A causes the reduction of unit cell sizes while the substitution of Sn^{+4} ions in the sublattice B causes the increase in these sizes. The substitution of ions of different size leads to the mechanical deformation of crystallites [7]. The methods of obtaining ceramic materials with specified grain sizes and homogeneity also affects their dielectric properties [8]. The conventional method of synthesis of BT ceramics requires the use of high temperature (about 1350°C) to carry out a solid phase reaction between barium carbonate and titanium dioxide powders. The use of such high temperatures results in low product purity and forms large particles (over 1 μm) with non-uniform grain size distribution [9]. Due to the high technological importance of this type of material and the demand for high quality, submicronic ceramic powders with a tailored size distribution, many researchers have focused on the development of low-temperature synthesis methods [10-13]. However, these novel synthesis methods are in general very expensive in comparison with the current powder manufacturing techniques. Recently it was found that high energy ball milling technique can be used for synthesis of nanocrystalline materials with perovskite structure [14-16]. This method has many advantages, such as simplicity, relative inexpensive production and applicability to many class of materials [17]. A high-energy ball milling of powders can greatly improve the reactivity of precursors, thereby reducing the temperature of BT structure formation during subsequent thermal treatment [18-19]. Also, as a consequence of high energy ball milling, the solid state reactions can promote in milling apparatus without any need for external

[1] PEDAGOGICAL UNIVERSITY, INSTITUTE OF TECHNOLOGY, 2 PODCHORĄŻYCH STR., 30-084 KRAKÓW, POLAND
[2] CRACOW UNIVERSITY OF TECHNOLOGY, FACULTY OF CHEMICAL ENGINEERING AND TECHNOLOGY, 24 WARSZAWSKA STR., 31-155 KRAKÓW, POLAND
[3] GDAŃSK UNIVERSITY OF TECHNOLOGY, DEPARTMENT OF MATERIALS ENGINEERING AND WELDING, FACULTY OF MECHANICAL ENGINEERING, 11/12 G.NARUTOWICZA STR., 80-233, GDAŃSK, POLAND

* Corresponding author: wojciech.bak@up.krakow.pl

heating. There are reports of receiving fine BT through intensive ball milling such as a planetary ball milling with long period of time [16,20-22]. However, this may result in serious drawbacks of high contamination due to wear of the balls and the vial. In this study, we demonstrate a rapid solid state mechanochemical synthesis of fine Sr^{+2} and Sn^{+4} ions modified $BaTiO_3$ powder, starting from a mixture of oxides. The influence of synthesis condition on microstructural, dielectric and ferroelectric properties of obtained solid solutions were investigated.

2. Experimental

The $BaTiO_3$ (BT) and the solid solutions $Ba_{0.9}Sr_{0.1}TiO_3$ (BS1T), $Ba_{0.9}Sr_{0.1}Ti_{0.9}Sn_{0.1}O_3$ (BS1TS1) and $Ba_{0.9}Sr_{0.1}Ti_{0.8}Sn_{0.2}O_3$ (BS1TS2) were prepared by solid state reaction using the high-energy ball milling technique. Barium oxide (Sigma Aldrich, 90%), TiO_2 (Sigma Aldrich, 99.7%), SrO (Sigma Aldrich, 99%) and SnO_2 (Sigma Aldrich, 99%) were used as the primary raw materials. All oxides were first heat treated to remove hydroscopic water. These precursors of stoichiometric quantity were hand-mixed in an agate mortar for two hours and subjected to high-energy milling in a Fritsch GmbH. *Pulverisette-6* planetary ball mill. The milling was performed in air with the vessel and balls (Ø = 10 mm) made of ZrO_2. The vessel was rotated at 550 rpm for 3 hours with a ball-to-powder weight ratio (BPR) of 20:1. As-milled powders were pressed into pellet discs with 8 mm in diameter and heat treated at 1200°C for 2h.

X-ray powder diffraction measurements for a phase analysis were performed on an X'Pert Phillips diffractometer using a CuK_α radiation (λ = 1.54178 Å) between 10° < 2 theta < 90° with step-width of 0.01°. The microstructure of the obtained polycrystalline samples was investigated with the use of a Hitachi S4700 cold-field-emission high-resolution scanning electron microscope with a microanalyses system Noran-Vantage. EDS (Energy-Dispersive X-Ray Spectroscopy) was applied to investigate the homogeneity of the composition. Dielectric measurements were carried out with the use of an Alpha-AN High Performance Frequency Analyzer system together with a cryogenic temperature control system – Quatro Cryosystem and WinDETA Novocontrol software, at frequency varying from 0.1 Hz to 10 MHz and at temperature ranging from –130°C to 250°C with 5°C step. The amplitude of measuring voltage was 1 V. Dielectric measurements were performed on polished polycrystalline discs after deposition of silver electrodes using nitrogen as a heating and cooling agent.

3. Results

3.1. Selection of mechanochemical process parameters

The synthesis of perovskite electroceramics by mechanochemical treatment on the example of BT are showed. Fig. 1 presents the X-ray diffractograms of the substrate powders at different times of high-energy mechanical treatment. After 10 minutes of milling, the disappearance of most diffraction reflections that correspond to the substrates structures is observed. This is due to the high fragmentation of grains and their partial amorphization. After 60 minutes of high-energy ball milling, small diffraction reflection at 2 Theta angles of 22.18, 31.6, 38.94, 45.26, 50.95 are visible, indicating the formation of the crystalline BT structure. With further milling, the diffractions reflections of the substrates disappear. After 180 minutes of high-energy processing of powders, only the BT structure is observed. In this paper, much more energetic milling of substrates, than those described in the literature was applied. This resulted in a significant reduction of the time necessary to obtain the desired BT structure. In addition, the use of substrates in the form of appropriate oxides also contributed to shortening the synthesis time. The process of decomposition of barium carbonate during high-energy ball milling is omitted, which significantly speeds up the formation of the product. Shortening the milling time has allowed to reduce the amount of impurities from grinding media that negatively affect the dielectric properties of polycrystalline samples. There are no diffraction reflections on the diffractogram of powder treated for 180 minutes indicating the presence of this type of contamination. Although, based on our previous studies focused on the synthesis of perovskite materials by mechanochemical treatment, it is known that under the described synthesis conditions this type of impurity may occur in an amount of about 1.85 percent [14].

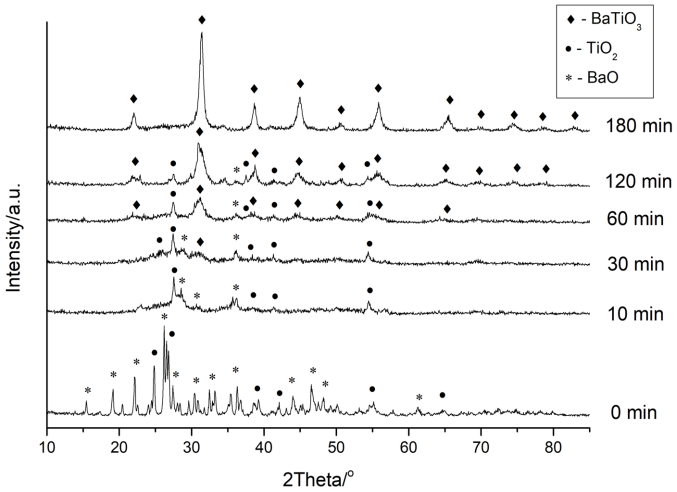

Fig. 1. XRD diffraction patterns of substrate powders after different time of mechanochemical processing

The mechanochemically prepared BT powder was characterized high grain homogeneity (Fig. 2a). The grain size was around 100 nm. Due to the fact, that the synthesis was proceeded at room temperature, the material does not contain sinters or unevenly grown grains. However, the high-temperature treatment resulted in a change in powder morphology (Fig. 2b). The sinters and agglomerates of varying sizes from 0.5 µm to 2.5 µm are clearly visible. The performed X-ray diffraction studies also confirmed the increase in crystallite size due to thermal treatment of the powder. Fig. 3 presents a comparison of X-ray diffraction pat-

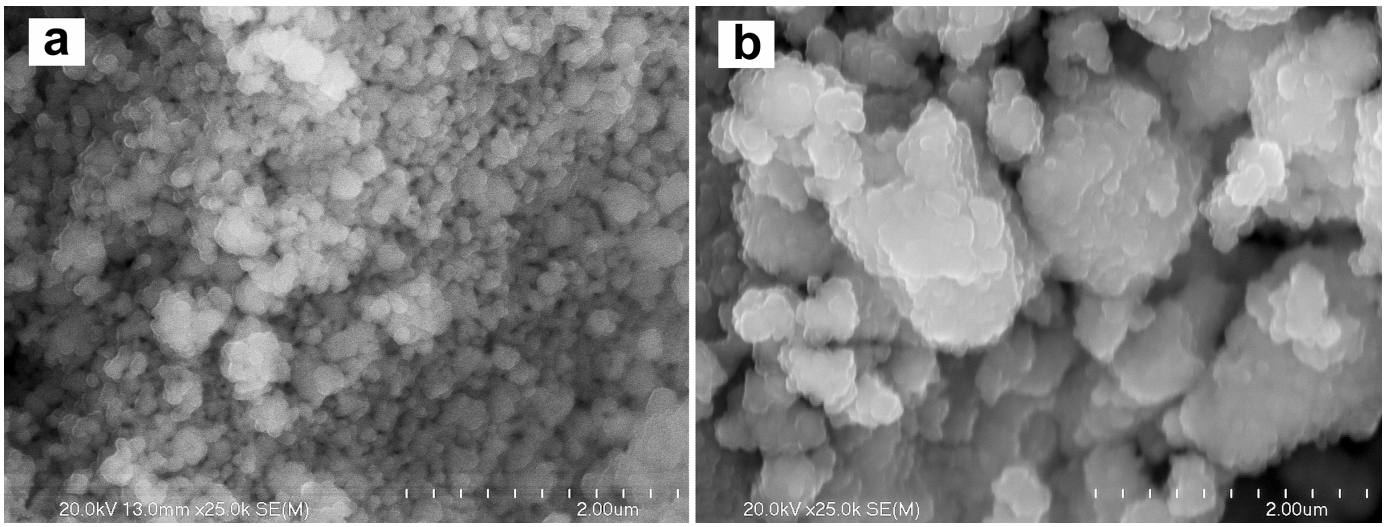

Fig. 2. SEM images of the BT powders prepared by mechanochemical synthesis method a) powder after 180 minutes of high-energy ball milling, b) powder after 180 minutes of high-energy ball milling and subsequent thermal treatment at 1200°C for 2 h

terns of mechanochemically prepared BT powder before and after the heat treatment process. Powders after thermal treatment had a much higher intensity of XRD reflections and their smaller half-widths than those of high-energy ball milling. This indicates on the improvement in crystallinity of the polycrystalline material.

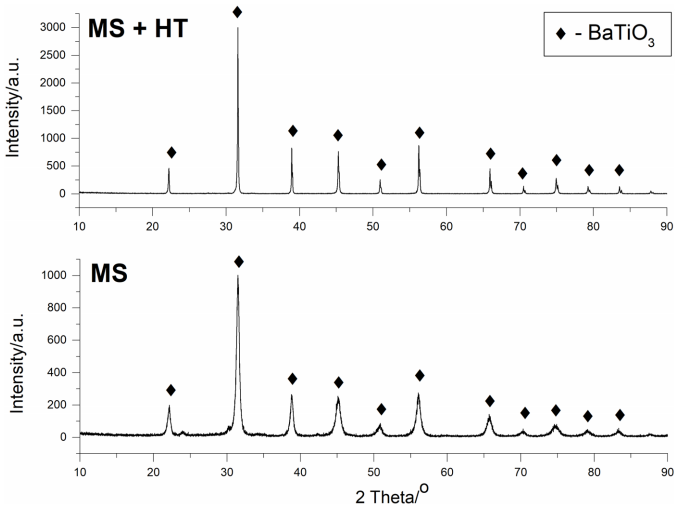

Fig. 3. Comparison of X-ray powder diffraction patterns of mechanochemically obtained BT powder, before (MS) and after (MS+HT) the thermal treatment process

heat treatment. Successful synthesis of appropriate solid solutions confirms a slight shift of the main diffraction reflections towards the lower 2 Theta angles. These shifts are caused by differences in the ionic radii of titanium and tin atoms.

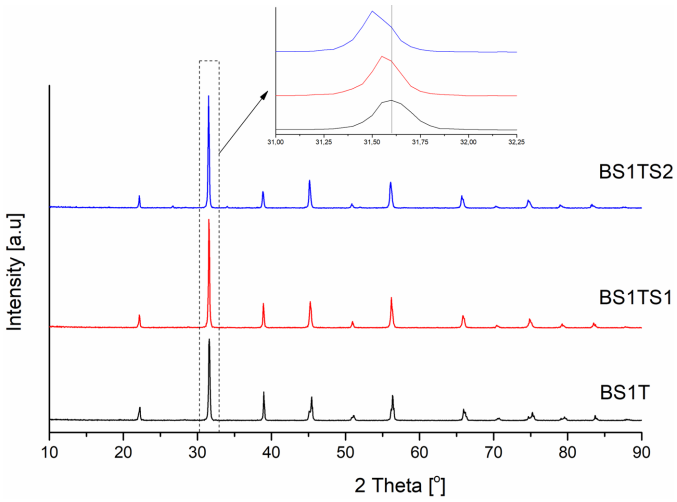

Fig. 4. Comparison of X-ray powder diffraction patterns of BS1T, BS1TS1 and BS1TS2 solid solutions powders prepared by mechanochemical synthesis method and subjected to subsequent heat treatment for 2 hours at 1200°C

3.2. Mechanochemical synthesis of solid solutions based on the $BaTiO_3$

The synthesis of BS1T, BS1TS1 and BS1TS2 solid solutions were performed in an analogous manner to the BT. In order to ensure the best possible dielectric properties, the mechanochemically obtained powders were subjected to a thermal treatment process for 2 hours at 1200°C. Fig. 4 presents a comparison of X-ray diffractograms of polycrystalline powders prepared by mechanochemical synthesis method and subjected to subsequent

The microstructure of BS1T, BS1TS1 and BS1TS2 solid solutions are shown in Fig. 5. It can be observed that the grain size is very widely distributed from more than 5 µm with irregularly shaped grains to submicron size with a change of Sn^{+4} ions content in BS1T ceramics. As the Sn^{+4} ions content is increased, the grain size distribution is narrowed down and the grains become more spherical also the proportion of the large grains in the overall microstructure decreases. The presence of agglomerates and sinters is clearly visible, this is due to the subsequent high-temperature treatment, especially in materials with a high content of Sn^{+4} ions.

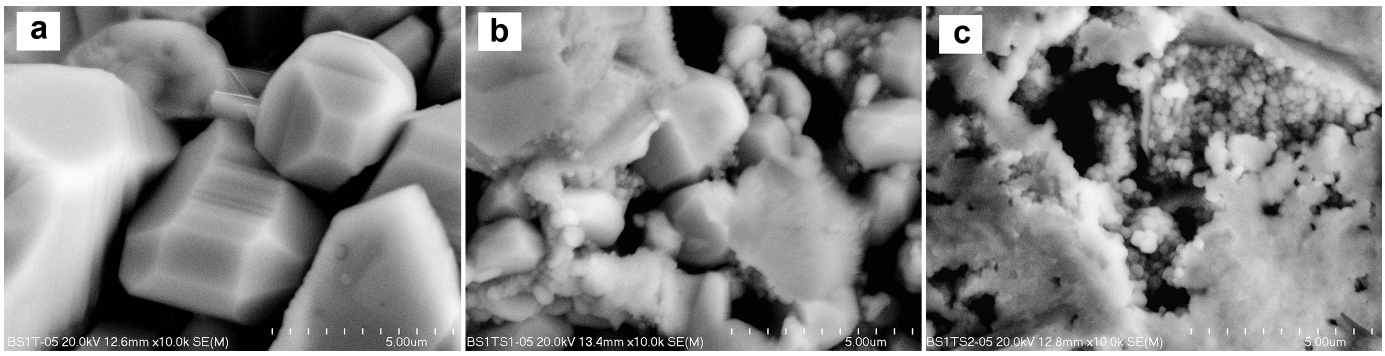

Fig. 5. The microstructure of BS1T (a), BS1TS1 (b) and BS1TS2 (c) solid solutions prepared by mechanochemical method and subjected to subsequent heat treatment for 2 hours at 1200°C

3.3. Dielectric properties of the ceramics

Dielectric properties of the investigated samples are described by the temperature dependences of the real part of the dielectric permittivity (ε') and frequency dependence of the imaginary part of the electric modulus (M''). Fig. 6 shows the dependences of $\varepsilon'(T)$ for the BT samples prepared by mechanochemical synthesis method and subjected to subsequent heat treatment for 2 hours at 1200°C. For the BT ceramic obtained by means synthesis at room temperature one can see the constant value (approx. 60) of the function $\varepsilon'(T)$ (plateau). The dielectric measurements of the sample obtained only by pressing the powder did not show any paraelectric – ferroelectric (PE-FE) phase transitions despite the presence the BT structure. This is due to the high powder disintegration and weak interaction between the grains. Only high temperature sinter allow to obtain a materials with higher density and ferroelectric properties. In this case the first order PE-FE phase transition occurs at 115°C. This transition is caused by the structural tetragonal – cubic change. With further temperature lowering, one can identify another maximum of $\varepsilon'(T)$ at 25°C, which is connected with transition to the orthorhombic structure. Below room temperature, no further maximum was observed related to the structural transition to the rhombohedral phase. For the BT polycrystalline sample obtained by the conventional high temperature synthesis method this rhombohedral phase occurs at –85°C [23].

Fig. 7 presents the real part of the dielectric permittivity ε' as the function of temperature for BS1T, BS1TS1 and BS1TS2 polycrystalline samples. For the BS1T ceramic the PE-FE phase transition appears at 90°C. The maximum value ε' for this sample in comparison to the BT one decreases by half. In the low temperature range (ferroelectric phase) one can see next maximum of $\varepsilon'(T)$ at –5°C. The phase transitions in the case of BS1T are diffused and additionally shifted to lower temperatures in comparison to the BT sample. This diffusivity and shift the temperature of the phase transitions is related to substitution of the Sr^{2+} ions in the A cationic sublattice. The substitution of the Sn^{4+} ions in the B cationic sublattice causes a further increase in the diffusion of the PE-FE phase transition. Simultaneously, the temperature of this phase transition lowers to the temperature of 25°C and –40°C for BS1TS1 and BS1TS2 samples, respectively.

It should be noted that for whole measuring frequency range (not shown here) the maximum of $\varepsilon'(T)$ occurs for the same temperatures. The temperature dependences of 1/ε'(T) for all investigated samples in paraelectric phase are presented in Fig. 8. The graphs of $1/\varepsilon'(T)$ for these samples confirm the compliance of Curie – Weiss law, which is given by the following equation: $\varepsilon' = C/(T - T_o)$, where: C is the Curie – Weiss constant, T_o – is the Curie

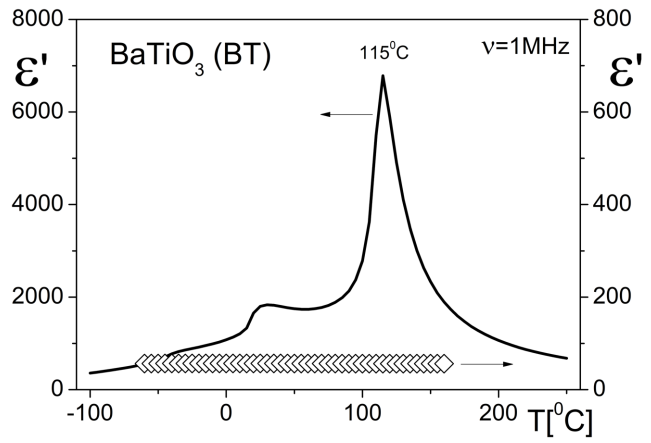

Fig. 6. The temperature dependence of the real part of the dielectric permittivity for the BT samples obtained by the mechanochemical methods (right Y axis) and subjected to subsequent heat treatment (left Y axis)

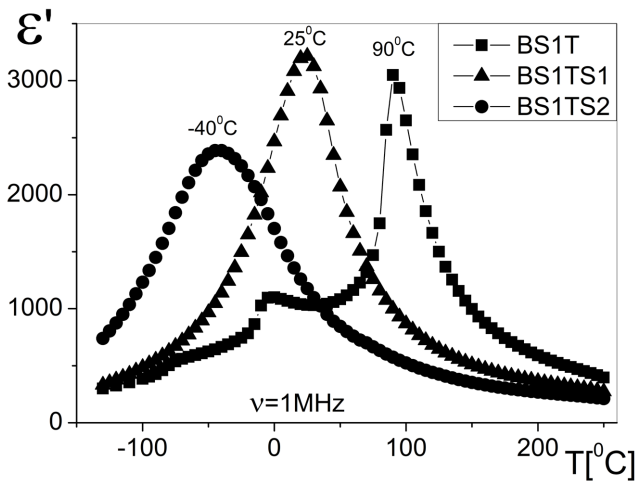

Fig. 7. The temperature dependence of the real part of the dielectric permittivity for solid solution samples at chosen frequency 1 MHz

– Weiss temperature. The constants C and T_o determined based on a linear regression procedure at frequency of 1MHz and showed on Fig. 8. The graphs of $1/\varepsilon'(T)$ does not reveal all the features of the diffuse phase transition (DPT). Therefore the following relation describing the temperature dependence of permittivity was proposed: $1/\varepsilon' = 1/\varepsilon'_m + A(T - T_m)^{\gamma}$ where: ε'_m is the maximum value of dielectric permittivity, T_m – temperature corresponding to ε'_m, A and ɣ are constants for chosen frequency. In the classical (first order) PE-FE phase transition the value of γ is close to 1, while in DPT it is close to 2. The values of γ for all investigated samples are presented in Fig. 9. For BT sample the value of $\gamma = 1.07$ indicates the classical PE-FE phase transition. Whereas in the case of BS1T, BS1TS1 and BS1TS2 samples two ranges of linear dependences above temperature T_m can be distinguished.

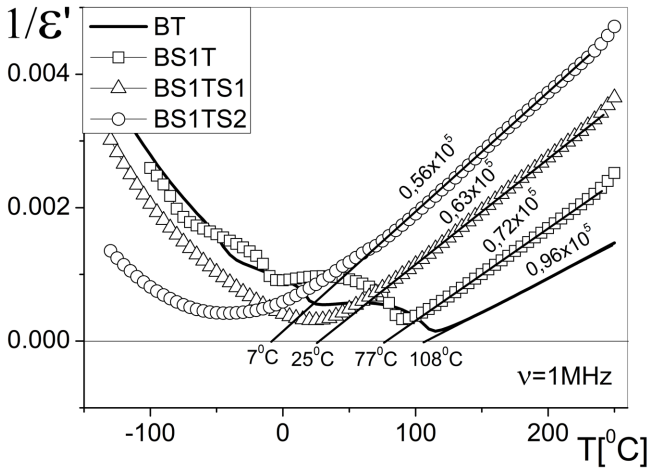

Fig. 8. The inverse of the real part of dielectric permittivity ($1/\varepsilon'$) as a function of temperature for BT, BS1T, BS1TS1 and BS1TS2 samples at chosen frequency 1 MHz

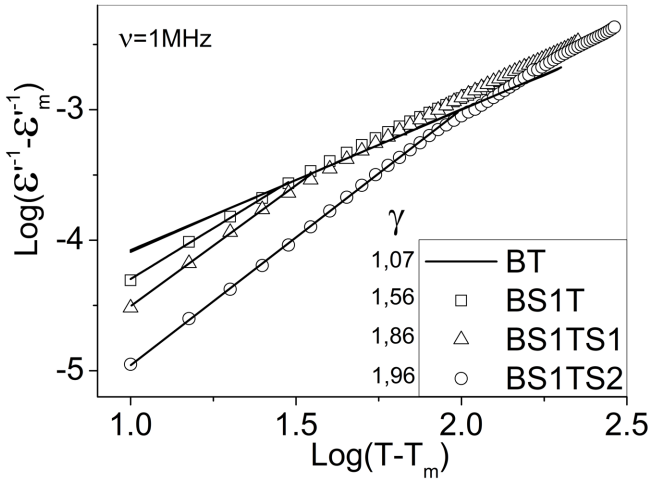

Fig. 9. The dependence of $\log(1/\varepsilon' - 1/\varepsilon'_m)$ on $\log(T - T_m)$ for BT, BS1T, BS1TS1 and BS1TS2 samples at chosen frequency 1 MHz

In the temperature range above 30°C, 35°C and 75°C from T_m for the samples BS1T, BS1TS1 and BS1TS2 respectively, γ values equal to 1.56, 1.86 and 1.96 confirms the diffusion of the PE-FE phase transition. The values of γ obtained at temperatures above 60°C, 120°C and 180°C from T_m for BS1T, BS1TS1 and BS1TS2 samples respectively reveal a slight diffusion of the PE-FE phase transition which is characteristic for BT sample. It can therefore be seen that the diffusion of the PE-FE phase transition in the cooling process begins at a temperature of about 150°C for BS1T, BS1TS1 and BS1TS2 samples.

The formalism of electric modulus is used to describe the phenomena of electric charge transport and dielectric relaxation in polycrystalline materials. The complex electric modulus is the reciprocal of the complex permittivity $M^* = 1/\varepsilon^*$ and corresponds to the relaxation of the electric field in the material when the electric displacement remains constant [24]. Fig. 10 show the imaginary part M'' as a function of frequency at chosen temperature 200°C (paraelectric phase) for all investigated samples. The magnitude of $M''(\nu_m)$ maximum increases with increase in substitution of Sr^{+2} and Sn^{+4} ions. Also, the maximum shifts systematically towards higher frequency side with increase in temperature (not shown here). These maximum corresponds to the so-called conductivity relaxation [25]. The characteristic relaxation time, $\tau = (2\pi\nu_m)^{-1}$ represent the time scale of transitions from short range to long range mobility of charge carriers with decreasing frequency. The low frequency side of the maximum represents the range of frequencies in which the ions are capable of moving long distances, whereas for the high frequency side, the ions are spatially confined to their potential wells and can execute only localized motion.

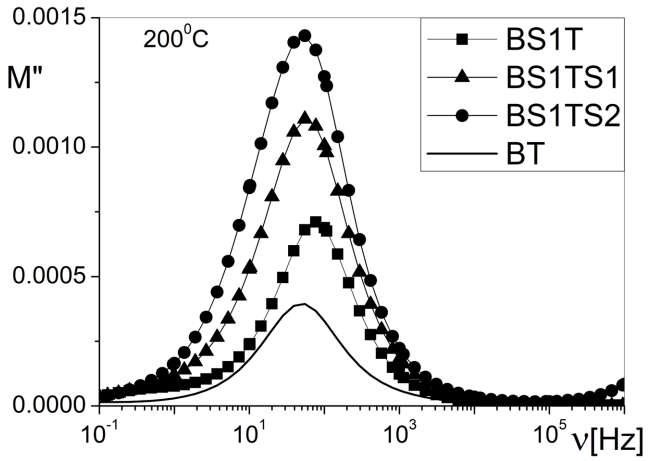

Fig. 10. Frequency dependence of the imaginary part of electric modulus (M'') for BT, BS1T, BS1TS1 and BS1TS2 samples at chosen temperature 200°C

The relaxation time, τ exhibits a thermally activated dependence. This generally follows the Arrhenius law: $\tau = \tau_o \exp(E_a/k_B T)$, where τ_o is the pre-exponential factor and E_a denotes the activation energy for dielectric relaxation. From Arrhenius plot (Fig. 11), the dc conductivity relaxation activation energy is computed, in the temperature range 100°C-250°C (paraelectric region) and found to be about 1 eV for all investigated samples. These values of the activation energies may be related to the electron excited process from the oxygen vacancy. Oxygen vacancies are most mobile charge carriers in oxide polycrystalline materials [26].

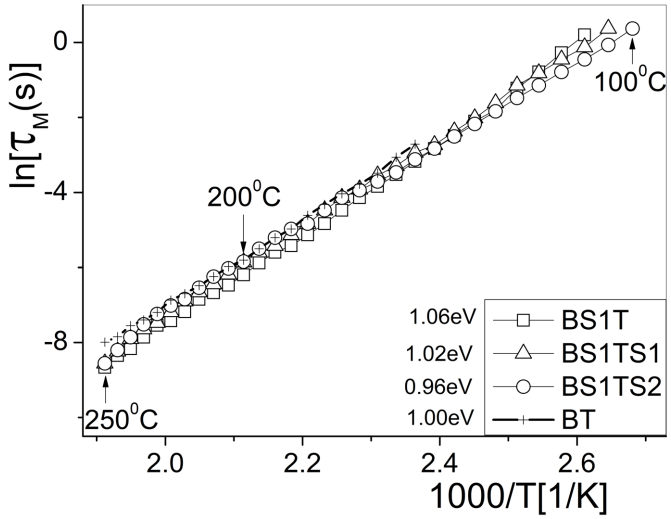

Fig. 11. Temperature dependence of relaxation times obtained from frequency dependent plots of M'' for BT, BS1T, BS1TS1 and BS1TS2 samples

4. Conclusions

The oxide polycrystalline materials on the basis of the $BaTiO_3$ are obtained with the use of a mechanochemical method and next a high temperature solid state reaction method (conventional). The influence of synthesis condition on microstructural, dielectric and ferroelectric properties of obtained solid solutions are presented. The use of high-energy ball milling significantly reduces the time of synthesis of BT, BS1T, BS1TS1 and BS1TS2 polycrystalline samples. It can be prepared at room temperature by 180 minute of high-energy ball milling of the stoichiometric mixture of the oxide powders. Mechanochemical synthesis method allows the production of BT polycrystalline samples with a grain size below 100 nm and exhibiting good homogeneity in terms of grain size. Shortening the time of the mechanochemical treatment reduces the costs of manufacturing such materials as well as reduces the amount of impurities from abrasive of grinding media. The Sr^{+2} and Sn^{+4} ions substitutions in the both cationic sublattices simultaneously generated the higher heterogeneity of structure which was confirmed by the X-ray measurements. The influence of Sn^{+4} ions content on the shape and size of grains of the tested samples was observed. With an increase in the content of Sn^{+4} ions, the grains become more spherical and the proportion of large grains in the overall microstructure decreases. The temperature dependences of the real part of the dielectric permittivity (ε') and frequency dependence of the imaginary part of the electric modulus (M'') for all investigated samples are presented. The diffusion of the paraelectric – ferroelectric phase transition for polycrystalline samples are described. The analysis of the temperature variation of M'' maximum indicates that the observed relaxation processes are thermally activated one and related to the electron excited process from the oxygen vacancy.

REFERENCES

[1] M.E. Lines, A.M. Glass, Principles and applications of ferroelectrics and related materials, Claredon Press, Oxford, (2001).
[2] J.F. Scott, Applications of modern ferroelectrics, Science **315**, 954-959 (2007).
[3] K. Tkacz-Śmiech, A. Koleżyński, W.S. Ptak, Ferroelectrics **237**, 57-64 (2000).
[4] K. Tkacz-Śmiech, A. Koleżyński, W. Jastrzębski, Ferroelectrics **315**, 73-81 (2005).
[5] M. Gabryś, C. Kajtoch, W. Bąk, B. Handke, F. Starzyk, Ferroelectrics **417**, 110-117 (2011).
[6] C. Kajtoch, W. Bąk, B. Garbarz-Glos, D. Ziętek, M. Gabryś, K. Stanuch, T. Czeppe, Ferroelectrics **464**, 15-20 (2014).
[7] Y. Tsur, T.D. Dunbar, C.A. Randall, J. Electroceram. **7**, 25-34 (2001).
[8] L.R. Prado, N.S. de Resende, R.S. Silva, S.M.S. Egues, G.R. Salazar-Banda, Chemical Engineering and Processing **103**, 12-20 (2016).
[9] G.H. Haertling, Ferroelectric ceramics: History and technology. Journal of the American Ceramic Society, **82** (4), 797-818 (1999).
[10] H.X. Bai, X.H. Liu, Materials Letters **100**, 1-3, (2013).
[11] H. Kageyama, Y. Oaki, Y. Takezawa, T. Suzuki, H. Imai, Journal of the Ceramic Society of Japan **121** (1412), 388-392 (2013).
[12] W.W. Wang, L.X. Cao, W. Liu, G. Su, W.X. Zhang, Ceramics International **39** (6), 7127-7134 (2013).
[13] A.V. Zanfir, G. Voicu, S.I. Jinga, E. Vasile, V. Ionita, Ceramics International **42** (1), 1672-1678 (2016).
[14] P. Dulian, W. Bak, K. Wieczorek-Ciurowa, C. Kajtoch, Materials Science-Poland **31** (3), 462-470 (2013).
[15] B.D Stojanovic, Journal of Materials Processing Technology **143**, 78-81 (2003).
[16] L.B. Kong, T.S. Zhang, J. Ma, F. Boey, Progress in Materials Science **53** (2), 207-322 (2008).
[17] P. Balaz, M. Achimovicova, M. Balaz, P. Billik, Z. Cherkezova-Zheleva, J.M. Criado, F. Delogu, E. Dutkova, E. Gaffet, F.J. Gotor, R. Kumar, I. Mitov, T. Rojac, M. Senna, A. Streletskii, K. Wieczorek-Ciurowa, Chemical Society Reviews **42** (18), 7571-7637 (2013).
[18] T. Sundararajan, S.B. Prabu, S.M. Vidyavathy, Materials Research Bulletin **47** (6), 1448-1454 (2012).
[19] R. Ashiri, RSC Advances **6** (21), 17138-17150 (2016).
[20] B.D. Stojanovic, A.Z. Simoes, C.O. Paiva-Santos, C. Jovalekic, V.V. Mitic, J.A. Varela, Journal of the European Ceramic Society, **25** (12), 1985-1989 (2005).
[21] V.V. Sydorchuk, V.A. Zazhigalov, S.V. Khalameida, K. Wieczorek-Ciurowa, Inorganic Materials **46** (10), 1126-1130 (2010).
[22] J.M. Xue, J. Wang, D.M. Wan, Journal of the American Ceramic Society **83** (1), 232-234 (2000).
[23] W. Bąk, P. Dulian, B. Garbarz-Glos, C. Kajtoch, K. Wieczorek-Ciurowa, Ferroelectrics **485,** 89-94 (2015).
[24] P.B. Macedo, C.T. Moynihan, R. Bose, Phys. Chem. Glasses, **13**, 171 (1972).
[25] M.P. Dasari, K. Sambasiva Rao, P. Murali Krishna, G. Gopala Krishna, Acta Physica Polonica A **119** (3), 387-394 (2011).
[26] H. Beltra, M. Prades, N. Maso, E. Cordoncillo, A.R. West, Journal of the American Ceramic Society, **94** (9), 2951-2962 (2011).